Dental Traumatology 2006; 22: 18–24

DENTAL TRAUMATOLOGY

Three-dimensional bone microstructures of the mandibular angle using micro-CT and finite element analysis: relationship between partially impacted mandibular third molars and angle fractures

Takada H, Abe S, Tamatsu Y, Mitarashi S, Saka H, Ide Y. Three-dimensional bone microstructures of the mandibular angle using micro-CT and finite element analysis: relationship between partially impacted mandibular third molars and angle fractures. Dent Traumatol 2006; 22: 18–24. © Blackwell Munksgaard, 2006.

Abstract – The mandibular angle is one of the areas of the mandible that are prone to bone fractures, and the presence of an impacted third molar has been found to be associated with increased risk of angle fractures. The factors involved in bone fractures are the amount and direction of load, and the biomechanical and anatomical properties of bone. In the present study, micro-focused X-ray computed tomography was performed to observe and analyze the three-dimensional (3D) bone microstructure of the mandibular angle, and finite element analysis was conducted to examine the relationship between angle fractures and the presence or absence of mandibular third molars. 3D bone microstructure showed no marked difference between mandibles with and without third molars. Finite element analysis showed that, in the mandible with a third molar, stress was concentrated around the root apex of the third molar, and was transmitted in a direction matching the clinical findings of angle fractures. The results obtained in this study suggest that the presence of an impacted third molar changes the concentration and transmission of stress in the mandible, thus increasing the risk of an angle fracture.

Hideki Takada[1], Shinichi Abe[1], Yuichi Tamatsu[2], Satoshi Mitarashi[1], Hideki Saka[1], Yoshinobu Ide[1]

[1]Department of Anatomy, Tokyo Dental College, Chiba, Japan; [2]Department of Neurology Gross Anatomy Section, Graduate School of Medical and Dental Science, Kagoshima University, Kagoshima, Japan

Key words: three-dimensional bone microstructure; micro-focused X-ray computed tomography; finite element analysis; partially impacted mandibular third molar; angle fracture

Hideki Takada, Department of Anatomy, Tokyo Dental College, 1-2-2 Masago, Mihama-ku, Chiba 261-8502, Japan
Tel.: +81 43 270 3759
Fax: +81 43 277 4010
e-mail: takada-h@mug.biglobe.ne.jp

Accepted 9 March, 2005

Several studies have documented the relationship between the presence of a third molar and fracture of the mandibular angle, which is one of the areas of the mandible that are prone to fracture. Clinico-statistical studies have confirmed that a third molar is often located on angle fracture lines (1–3). Also, there are some papers describing that the risk of angle fracture is about two to four times greater for mandibles with third molars than those without (2–5). The risk of angle fracture is even higher for mandibles with impacted third molars (1, 3, 5).

The factors related to bone fractures include the amount and direction of load, biomechanical properties of bone, and anatomical properties (1, 3, 4, 6–8). Takeuchi et al. (8) conducted a mechanical study of the mandible using the finite element method, and showed that when load was applied to the angle, a major area of destruction was in the mandibular ramus and the angle. However, they did not investigate the effects of presence of a third molar. Reitzik et al. (9) conducted a mechanical study using vervet monkey mandibles, and reported that the presence of third molars increased the risk of angle fractures. Nakajima et al. (10) conducted a two-dimensional imaging study on the internal structure of the mandible from the mandibular ramus to the angle, and reported that the ratio of trabecular bone was higher for the angle than for the ramus, and that the thickness of the trabecular bone was greater in the angle than in the ramus. However, there have been no detailed anatomical studies of angle fractures, and the factors involved in angle fractures remain unclear.

Micro-focused X-ray computed tomography (micro-CT) is widely used to observe and analyze internal structures in a non-invasive manner (11, 12). Mechanical studies based on digital data obtained by micro-CT and other techniques (13, 14) have shown that such findings can be used to predict the risk of bone fractures (15).

In the present study, we performed micro-CT to assess differences in three-dimensional (3D) microstructures of mandibles with or without impacted third molars. Also, we performed mechanical analysis based on the finite element method, to identify the factors that increase the risk of angle fracture in mandibles with impacted third molars.

Materials and methods

We used 15 formalin-fixed Japanese adult male cadavers stored by the Department of Anatomy of Tokyo Dental College. The third molar was absent in 10 sides of eight cadavers, and the third molar was present in 10 sides of seven cadavers (Table 1). Based on Pell and Gregory's classification system for third molar impaction (16), we selected mandibles with third molars that had class B occlusal position and were not subjected to occlusal pressure. All mandibles had first and second molars, and occlusion was maintained.

The mandible was imaged by micro-CT (KMS-755; Kashimura, Tokyo, Japan) after removing only the soft tissue. The mandibular plane was set orthogonal to the sample stage, and imaging was performed under the following conditions: tube voltage, 65 kV; tube current, 100 μA; slice width, 50 μm. Raw data were obtained by rotating the sample stage 360 degrees. Then, slice images were prepared using multi-tomographic image reconstruction software (MultiBP; Imagescript, Tokyo, Japan).

Table 1. Materials

No	Age: Mandibles without third molars	Age: Mandibles with third molars
1	40	43
2	47	55
3	56	58
4	57	62
5	62	68
6	69	70
7	Unknown	Unknown
8	Unknown	

For observation and analysis of reconstructed 3D images, we used 3D trabecular structure analysis software (TRI/3D-BON; RATOC System Engineering, Tokyo, Japan). Reconstructed 3D images were prepared from slice images using the volume rendering method, to analyze the microstructure of the bone around the root apex of impacted third molars and the equivalent area in mandibles without third molars. For mandibles without third molars, an area 10.0 mm distal to the second molar was selected as the region of interest, based on the mesiodistal crown diameter of mandibular third molars (17). For mandibles with third molars, the root apex of the third molar was selected as the region of interest. The volume of interest (VOI) was a $5.0 \times 5.0 \times 5.0\ mm^3$ ($100 \times 100 \times 100$ voxel) cube at the buccolingual center parallel to the inferior border of the mandible and touching the superior border of the mandibular canal (Fig. 1a,b).

The following parameters were measured: bone volume fraction (bone volume/tissue volume, BV/TV%), trabecular thickness (Tb.Th mm), trabecular number (Tb.N/mm), trabecular separation (Tb.Sp mm), fractal dimension, connectivity density (CD/mm^3), trabecular bone pattern factor (TBPf/mm), structure model index (SMI), and degree of anisotropy (DA). BV/TV and Tb.Th were directly measured, whereas Tb.N and Tb.Sp were calculated as derived parameters based on the parallel plate model proposed by Parfitt et al. (18). The other parameters were directly determined from 3D data. An unpaired *t*-test was used to compare intergroup differences between mandibles with and without partially impacted third molars. $P < 0.05$ was considered to indicate statistical significance.

Finite element analysis was performed using slice images obtained by micro-CT and stress analysis

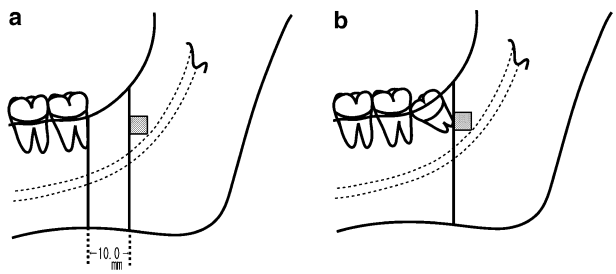

Fig. 1. The volume of interest (VOI) observed and analyzed in three-dimensional bone microstructures. (a) Mandibles without third molars, (b) Mandibles with partially impacted third molars, and ■ VOI.

software based on a finite element method (TRI/3D-FEM; RATOC System Engineering). We prepared a finite element model of a region from the distal border of the second molar to the posterior border of the mandibular ramus, using one 57-year-old cadaver without a third molar and one 55-year-old cadaver with a third molar.

As preprocessing of 3D images for finite element analysis, after removing noise, each image was downsized and subjected to binarization based on a threshold value obtained by discriminant analysis. After labeling, a finite element model was prepared by mapping eight-noded cube-shaped elements. The number of nodes and elements was approximately 550 000 and 750 000 respectively.

The models were prepared using bone and teeth with linear, elastic and isotropic properties based on published values. Young's modulus and Poisson's ratio were as follows: bone, 15 GPa and 0.3, respectively (19, 20); teeth, 40 GPa and 0.3, respectively (8). The fixed boundary conditions were all nodes on the posterior border of the mandibular ramus and on the frontal section of the body of the mandible posterior to the second molar. Load was applied to the center of the body on the linear line extending from the anterior border of the ramus to the inferior border of the body. A load of 2000 N (8) was applied perpendicular to the buccal surface of the mandibular body (Fig. 2).

Stress distribution was investigated based on color differences in von Mises equivalent stress (15, 21). Also, in order to objectively assess the correspondence between stress transmission and clinical angle fracture lines, the VOI was established for each specimen. First, a 12.0-mm region was established mesiodistally around the line extending from the anterior border of the ramus to the inferior border of the body. The VOI was the area surrounded by the inferior border of the body and the plane formed by extending the buccolingual alveolar bone crests to the posterior border of the ramus (Fig. 3). By calculating the stress value of each element, a histogram was prepared to investigate stress distribution, and mean and standard deviation were calculated.

Results

For mandibles with or without third molars, in the area above the mandibular canal, trabecular bone was mainly aligned vertically from the alveolar crest to the mandibular canal. In the area below the mandibular canal, trabecular bone was aligned horizontally connecting the buccal and lingual cortical bone. In the VOI, the trabecular bone consisted of plate and rod-like trabeculae (Fig. 4). There was no marked intergroup difference in bone structure.

Analysis of 3D bone microstructure (Table 2) showed that no significant difference in any of the parameters between mandibles without third molars and mandibles with partially impacted third molars.

In terms of the distribution of von Mises equivalent stress on sagittal sections, in the mandible without a third molar, stress was transmitted along the mandibular canal towards the body, and was distributed diffusely. However, for the mandible with a third molar, stress was concentrated around the root apex of the third molar. When the sagittal section was superimposed with the partially impacted third molar, stress was clearly concentrated at the root apex (Fig. 5b2). Also, stress was transmitted towards the base of the mandible and the angle, thus matching the clinical findings associated with angle fractures. Furthermore, stress was distributed in the trabecular bone near the neck of third molar (Fig. 5).

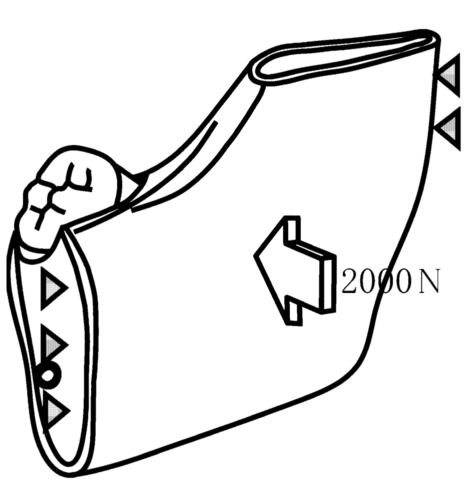

Fig. 2. The loading and fixed boundary condition.

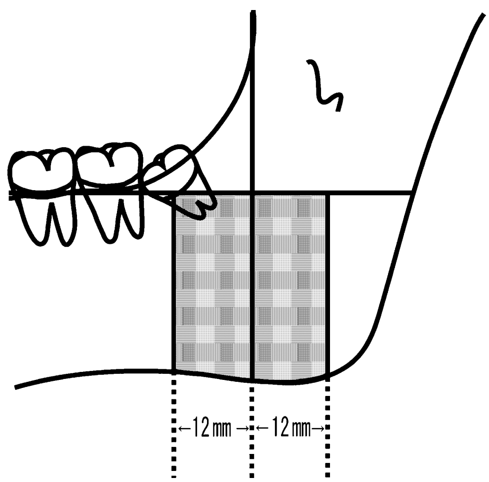

Fig. 3. The volume of interest analyzed in von Mises equivalent stress distribution.

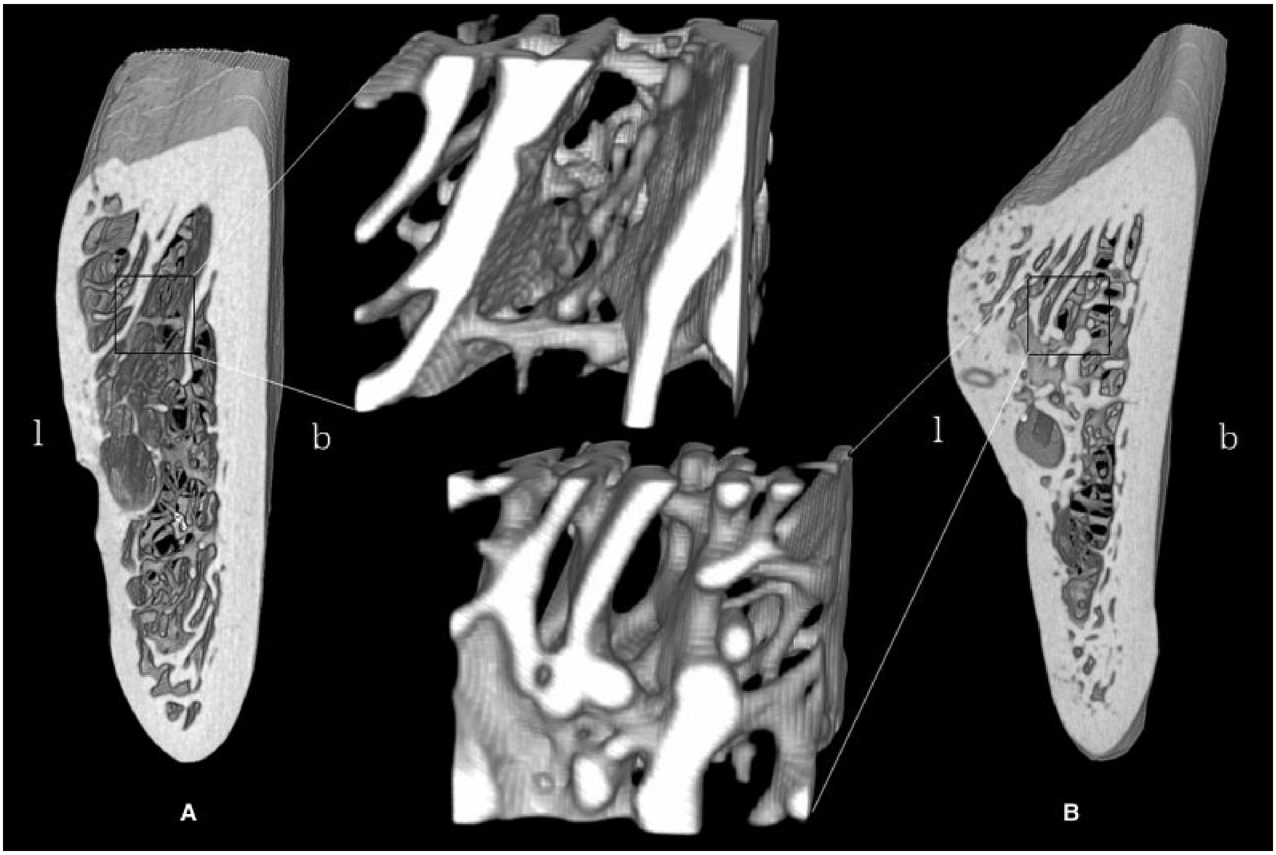

Fig. 4. Reconstructed three-dimensional images at the volume of interest. (A) Mandible without a third molar and (B) mandible with a partially impacted third molar. b: Buccal side, l: lingual side.

Table 2. Three-dimensional bone microstructure analysis

	Mandibles without third molars ($n = 10$)	Mandibles with third molars ($n = 10$)
BV/TV (%)	36.08 ± 16.66	32.77 ± 5.38
Tb.Th (mm)	0.40 ± 0.15	0.35 ± 0.07
Tb.N (/mm)	0.87 ± 0.13	0.95 ± 0.08
Tb.Sp (mm)	0.77 ± 0.29	0.71 ± 0.07
FD	2.21 ± 0.05	2.26 ± 0.06
CD (/mm^3)	0.75 ± 0.15	0.88 ± 0.43
TBPf (/mm)	−0.19 ± 1.49	0.19 ± 0.71
SMI	1.81 ± 0.43	1.75 ± 0.17
DA	1.55 ± 0.22	1.49 ± 0.15

Values are given as mean ± SD.
BV/TV, bone volume fraction; Tb.Th, trabecular thickness; Tb.N, trabecular number; Tb.Sp, trabecular separation; FD, fractal dimension; CD, connectivity density; TBPf, trabecular bone pattern factor; SMI, structure model index; DA, degree of anisotropy.

In terms of the distribution of von Mises equivalent stress on frontal sections near the anterior border of the ramus, in the mandible without a third molar, stress was not transmitted towards the base of the mandible. However, in the mandible with a third molar, stress was transmitted from the root apex to the base of the mandible (Fig. 6).

As to the stress distribution in the VOI, stress greater than 20 MPa was observed in the mandible with a third molar. Also, average von Mises equivalent stress was 9.76 ± 6.89 MPa in the mandible without a third molar and 14.93 ± 7.62 MPa in the mandible with a third molar (Fig. 7).

Discussions

Observation of reconstructed 3D images

The shape of trabecular bone is seemed to be determined by functional pressure (22). Shibuya et al. (11) investigated the trabecular structure of the mandible, and reported that the trabecular number increased, trabecular thickness narrowed, and trabeculae became structurally uniform following teeth loss. Also, it is known, in the area from the mandibular ramus to the angle, a large amount of tension is applied to the masseter muscle, medial pterygoid muscle and temporal muscle to elevate the mandible during mastication. These facts suggest that occlusal pressure and muscular tension can affect the shape of trabecular bone.

In the area examined in the present study, there was no marked difference in the trabecular structure between mandibles with and without partially

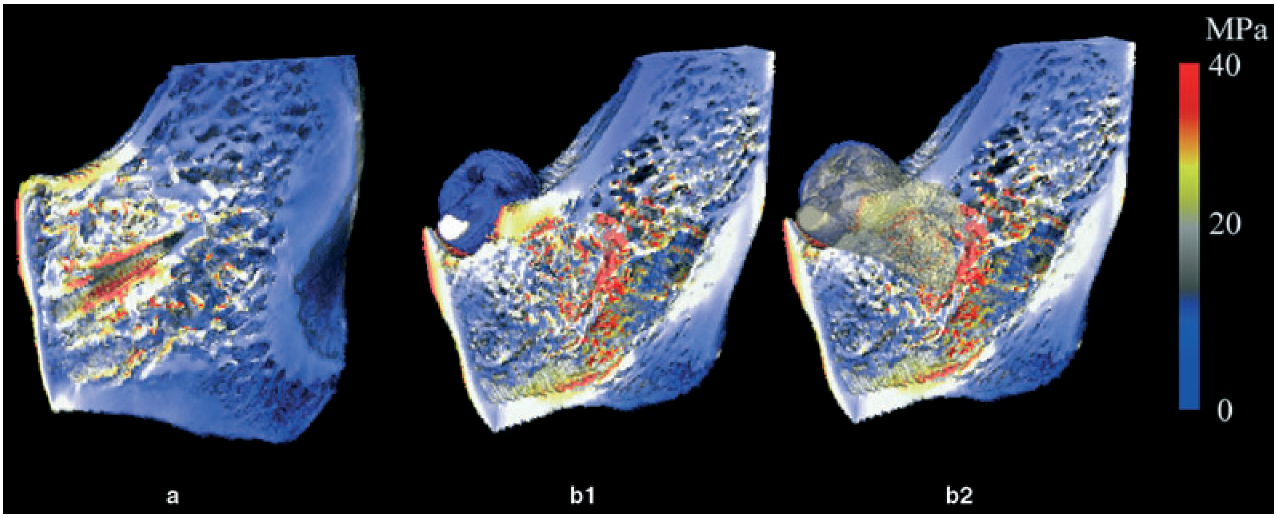

Fig. 5. Contour plot of von Mises equivalent stress distribution on sagittal sections. (a) The mandible without a third molar, (b1) The mandible with a partially impacted third molar, and (b2) The image of mandible with a partially impacted third molar superimposed with a third molar.

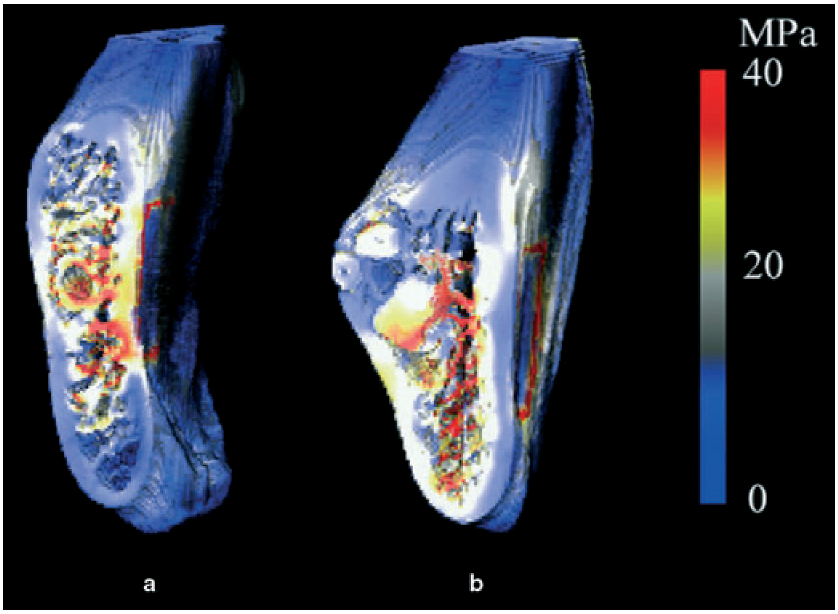

Fig. 6. Contour plot of von Mises equivalent stress distribution on frontal sections near the anterior border of the mandibular ramus. (a) The mandible without a third molar and (b) the mandible with a partially impacted third molar.

impacted third molars. The reason for this may be that all mandibles with or without third molars were dentulous, with the result that occlusal pressure was not applied to the partially impacted third molars. Also, muscular tension applied to the third molar region was not affected by the presence or absence of partially impacted third molars. Therefore, these findings suggest that partially impacted third molars do not affect the structure of the surrounding trabecular bone.

Three-dimensional bone microstructure analysis

Bone density and bone microstructure determine the mechanical properties of bone (23, 24). By analyzing bone microstructure, it is possible to predict bone strength (23–26). Bone volume (23, 24), trabecular anisotropy (23–25) and connectivity (24, 25) are thought to be important factors in bone strength.

In a study of the relationship between bone fracture and bone microstructure, Ito et al. (27) found a significant decrease in BV/TV and an increase in Tb.Sp in patients with compressed spinal fracture. In a study of the morphology of trabecular bone, Ulrich et al. (28) found that plate-like trabeculae are stronger than rod-like trabeculae. In osteoporosis, holes are created in plate-like trabeculae which undergo a change to rod-like trabeculae, thus lowering bone strength (29) and increasing the risk of bone fracture (30).

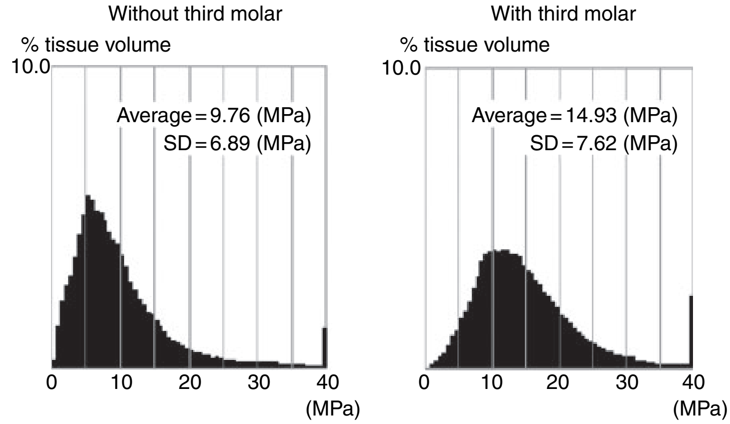

Fig. 7. Histograms representing von Mises equivalent stress distribution in the volume of interest (VOI) for the 2000 N load. The mean and standard deviation calculated for each element in the VOI are indicated as well.

BV/TV has been used as a parameter for bone volume, DA for anisotropy, CD and TBPf for connectivity, and SMI for trabecular morphology. However, in the present study, there was no marked difference in any of these parameters between the mandibles with and without impacted third molars. The reason for this was that, as mentioned above, the presence of a partially impacted third molar does not affect trabecular structure, which is a factor in bone strength.

Finite element analysis

In the present study, the distribution and localization of stress at the trabecular level was visually assessed (30). We found that, in the mandible with a third molar, stress was concentrated around the root apex, and was transmitted in a direction matching clinical fracture lines.

Stress is believed to concentrate in the following three types of areas: areas bearing load from another area; areas with morphological characteristics such as furrowing, sharp angles or irregularity; and areas with different elastic coefficients (31). The area surrounding the root apex of impacted third molars satisfies all of these conditions, suggesting that the root apex of impacted third molars is prone to stress concentration. Also, concentrated stress is believed to be transmitted to the base and angle of the mandible. Furthermore, in the mandible without a third molar, stress is distributed diffusely because of the lack of a structure where stress could concentrate.

Fuselier et al. (2) and Meisami et al. (3) conducted clinicostatistical studies to investigate the relationship between angle fracture and third molar impaction, and reported that the risk of angle fracture was high for mandibles with partially impacted third molars. The reason for this is that eruption of a partially impacted third molar ruptures the internal and external oblique ridge, thus decreasing the strength of the mandibular angle. In the present study, we examined mandibles with partially impacted third molars, and the results showed that stress was distributed in trabecular bone near the neck of the third molar. These findings suggest that a ruptured internal and external oblique ridge caused by eruption of a partially impacted third molar is involved in angle fracture.

Conclusion

We assessed differences in 3D bone microstructures, and used the finite element method to examine mechanical differences between mandibles with and without partially impacted third molars. In terms of 3D bone microstructures, there were no marked differences between mandibles with and without partially impacted third molars. The results of finite element analysis showed that, in mandible with partially impacted third molar, stress was concentrated around the root apex of the third molar, and was transmitted in a direction matching clinical angle fractures. These findings suggest that the presence of an impacted third molar increases the risk of angle fracture by altering the concentration and transmission of stress in the mandible.

References

1. Ugboko VI, Oginni FO, Owotade FJ. An investigation into the relationship between mandibular third molars and angle fractures in Nigerians. Br J Oral Maxillofac Surg 2000;38:427–9.
2. Fuselier JC, Ellis EE III, Dodson TB. Do mandibular third molars alter the risk of angle fracture? J Oral Maxillofac Surg 2002;60:514–8.
3. Meisami T, Sojat A, Sandor GKB, Lawrence HP, Clokie CML. Impacted third molars and risk of angle fracture. Int J Oral Maxillofac Surg 2002;31:140–4.
4. Lee JT, Dodson TB. The effect of mandibular third molar presence and position on the risk of an angle fracture. J Oral Maxillofac Surg 2000;58:394–8.

5. Ma'aita J, Alwrikat A. Is the mandibular third molar a risk factor for mandibular angle fracture? Oral Surg Oral Med Oral Pathol Oral Radiol Endod 2000;89:143–6.
6. Weiss L. Static loading of the mandible. Oral Surg Oral Med Oral Pathol 1965;19:253–62.
7. Halazonetis JA. The 'weak' regions of the mandible. Br J Oral Surg 1968;6:37–48.
8. Takeuchi S, Oka T, Ichikawa Y, Kawamoto T. Experimental and numerical studies on fracture of human mandible: 2. Investigation on the three-dimensional finite element model and fracture of human mandible. Jpn J Oral Maxillofac Surg 1985;31:248–63.
9. Reitzik M, Lownie JF, Cleaton-Jones P, Austin J. Experimental fractures of monkey mandibles. Int J Oral Surg 1978;7:100–3.
10. Nakajima K, Onoda Y, Okada M, Abe S, Ide Y. A study of the internal structure of the mandibular ramus in Japanese. Bull Tokyo Dent Coll 1998;39:57–65.
11. Shibuya E, Hara T, Ide Y. An internal structure in mental region of human jaw bone using micro-CT. J Jpn Soc Bone Morphom 2001;11:37–46 (in Japanese).
12. Oi T, Saka H, Ide Y. Three dimensional observation of pulp cavity in the maxillary first premolar using micro-CT. Int Endod J 2004;37:46–51.
13. van Rietbergen B, Muller R, Ulrich D, Ruegsegger P, Huiskes R. Tissue stresses and strain in trabeculae of a canine proximal femur can be quantified from computer reconstructions. J Biomech 1999;32:165–73.
14. Verdonschot N, Fennis WMM, Kuijs RH, Stolk J, Kreulen CM, Creugers NHJ. Generation of 3-D finite element models of restored human teeth using micro-CT techniques. Int J Prosthodont 2001;14:310–5.
15. Ulrich D, van Rietbergen B, Laib A, Ruegsegger P. Load transfer analysis of the distal radius from in-vivo high-resolution CT-imaging. J Biomech 1999;32:821–8.
16. Pell GJ, Gregory GT. Report on a ten-year study of a tooth division technique for the removal of impacted teeth. Am J Orthod 1942;28:660–6.
17. Berkovitz BKB, Holland GR, Moxham BJ. Oral anatomy, embryology and histology, 3rd edn. St Louis, MO: Mosby; 2002. p. 8–57.
18. Parfitt AM, Drezner MK, Glorieux FH, Kanis JA, Malluche H, Meunier PJ et al. Bone histomorphometry: standarization of nomenclature, symbols, and units. Report of the ASBMR histomorphometry nomenclature committee. J Bone Miner Res 1987;2:595–610.
19. Hara T, Takizawa M, Sato T, Ide Y. Mechanical properties of buccal compact bone of the mandibular ramus in human adults and children: relationship of the elastic modulus to the direction of the osteon and the porosity ratio. Bull Tokyo Dent Coll 1998;39:47–55.
20. Turner CH, Rho J, Takano Y, Tsui TY, Pharr GM. The elastic properties of trabecular and cortical bone tissues are similar: results from two microscopic measurement techniques. J Biomech 1999;32:437–41.
21. Geramy A, Sharafoddin F. Abfraction: 3D analysis by means of the finite element method. Quintessence Int 2003;34:526–33.
22. Huiskes R, Weinans H, Grootenboer HJ, Dalstra M, Fudala B, Slooff TJ. Adaptive bone-remodeling theory applied to prosthetic-design analysis. J Biomech 1987;20:1135–50.
23. Ulrich D, van Rietbergen B, Laib A, Ruegsegger P. The ability of three-dimensional structural indices to reflect mechanical aspects of trabecular bone. Bone 1999;25:55–60.
24. Goulet RW, Goldstein SA, Ciarelli MJ, Kuhn JL, Brown MB, Feldkamp LA. The relationship between the structural and orthogonal compressive properties of trabecular bone. J Biomech 1994;27:375–89.
25. Odgaard A. Three-dimensional methods for quantification of cancellous bone architecture. Bone 1997;20:315–28.
26. Ito M, Nishida A, Koga A, Ikeda S, Shiraishi A, Uetani M et al. Contribution of trabecular and cortical components to the mechanical properties of bone and their regulating parameters. Bone 2002;31:351–8.
27. Ito M, Nakamura T, Matsumoto T, Tsurusaki K, Hayashi K. Analysis of trabecular microarchitecture of human iliac bone using microcomputed tomography in patients with hip arthrosis with or without vertebral fracture. Bone 1998;23:163–9.
28. Ulrich D, Hildebrand T, van Rietbergen B, Muller R, Ruegsegger P. The quality of trabecular bone evaluated with micro-computed tomography, FEA and mechanical testing. In: Lowet G, Ruegsegger P, Weinans H, Meunier A, editors. Bone research in biomechanics. Amsterdam: IOS Press; 1997. p. 97–112.
29. Muller R, van Campenhout H, van Damme B, van Der Perre G, Dequeker J, Hildebrand T et al. Morphometric analysis of human bone biopsies: a quantitative structural comparison of histological sections and micro-computed tomography. Bone 1998;23:59–66.
30. Borah B, Gross GJ, Dufresne TE, Smith TS, Cockman MD, Chmielewski PA et al. Three-dimensional microimaging (MRμI and μCT), finite element modeling, and rapid prototyping provide unique insights into bone architecture in osteoporosis. Anat Rec 2001;265:101–10.
31. Caputo AA, Standlee JP. Biomechanics in clinical dentistry. Chicago: Quintessence Publishing; 1987. p. 13–28.